NEUTRONIC DESIGN STUDIES FOR THE SPALLATION NEUTRON SOURCE (SNS)

L. A. Charlton, J. M. Barnes, J. O. Johnson, and T. A. Gabriel
Oak Ridge National Laboratory
P. O. Box 2008
Oak Ridge, TN 37831-6363
(423) 574-0628

ABSTRACT

Neutronics analyses are now in progress to support initial selection of target system design features, materials, geometry, and component sizes for the proposed Spallation Neutron Source (SNS). Calculations have been performed to determine the neutron, proton, heavy ion, and gamma-ray flux spectra as a function of time, energy, and space for the major components of the target station (target, moderators, reflectors, etc.). These analyses were also performed to establish an initial set of performance characteristics for the neutron source. The methodology, reference performance characteristics, and results of initial optimization studies involving moderator poison plate location, target material performance, reflector performance, moderator position and premoderator performance for the target system are presented in this paper.

I. INTRODUCTION

In many areas of physics, materials and nuclear engineering, it is extremely valuable to have a very intense source of neutrons so that the structure and function of materials can be studied. One facility proposed for this purpose is the Spallation Neutron Source (SNS). This facility will consist of two parts: 1) a high-energy (~1 GeV) and high powered (~1 MW) proton accelerator and accumulator ring, and 2) a target station which converts the protons to low-energy (≤ 2 eV) neutrons and delivers them to the neutron scattering instruments.

This paper deals with the second part of the facility, i.e., the design and development of the SNS target station and the scientifically challenging issues. Many scientific and technical disciplines are required to produce a successful target station. These include engineering, remote handling, neutronics, materials, thermal hydraulics, and instrumentation. In this paper initial neutronic analysis calculations which simulate the spallation process and the moderation of the neutrons to low energy will be described. These calculations serve to establish facility characteristics and to allow optimization of the design. In the following sections, the methodology will be briefly described, followed by a presentation of the expected SNS neutron production performance. Results of initial optimization studies involving moderator poison plate location, target material performance, reflector performance, moderator position and premoderator performance for the target system will be shown.

II. METHODOLOGY

The neutronic behavior of the target system can be obtained by using Monte Carlo techniques to track the progress of various subatomic particles as they proceed through the target. For the work presented here the codes HETC[1] and MCNP[2] were used. The codes were coupled in order to provide the proper source for the low-energy (≤ 20 MeV) MCNP calculations. Various parameters were calculated to measure the neutronic performance of the target design. The two parameters which were most often tracked in the study reported below were the neutron current (J) passing into the neutron beam channels which lead to the experimental area and the time width (W) of the beam channel neutron pulse. For this source characterization and optimization study, a proton energy of 1.0 GeV, a power of 1 MW, a repetition rate of 60 Hz, and a proton pulse width of 0.5 μs was assumed.

Two target station geometries have been used for the initial evaluation of the SNS target system performance.

The first was used for calculations of the neutron flux leaving the moderator face and the energy deposition in the mercury target which did not require a detailed representation of the outer target station structure. This model has a beryllium reflector outer volume with dimensions of 900 mm x 900 mm x 1008 mm. The beryllium encloses a proton beam channel with dimensions 120 mm x 320 mm. A 640 mm long mercury target is placed at the end of this channel. The mercury target has a half cylinder on the front (where the proton beam enters) with radius of 50 mm. Downstream from the half cylinder was a section with rectangular cross section width of 300 mm and a height varying from 100 mm to 150 mm at the extreme downstream end. Moderators measure 120 mm x 150 mm x 50 mm with the smaller dimension being the thickness (i.e., the distance measured perpendicular to the viewed moderator face) and the largest dimension being the height. A view of the first model from outside the beryllium reflector is shown in Figure 1.

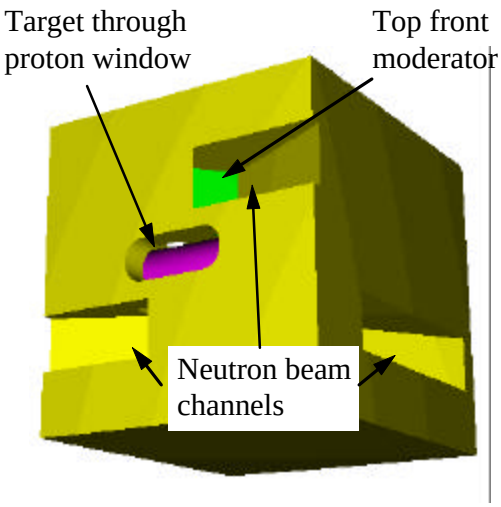

Figure 1. Outside of initial target station model.

A second geometry model was constructed to determine the energy deposition, material damage, activation, radiation flux spectra, and shielding requirements for the entire target station including the biological shielding. In this geometry, the mercury target was represented with a simplified model since the detailed model already existed for analysis in the first model. The moderator assemblies and associated neutron beam tube design from the initial target station model was incorporated into this model. A schematic diagram of the second model is given in Figure 2 along with a blowup of the central target region. Table 1 lists the material compositions associated with the various regions identified in Figure 2. On this scale, the beam tubes are barely visible on the outer surface of the exterior concrete biological shield. The full target station model is shown in Figure 3 with the outer concrete, iron, stainless steel vessel and the nickel and beryllium reflectors removed. The upper and lower beam tubes can be seen together with the cadmium decoupler which surrounds the beam channels and the moderators. To determine if the two models were consistent with respect to each other, the neutron output from the moderator faces from the two models were calculated. Initial comparisons indicated agreement within ~10% for the two models.

III. PERFORMANCE OF THE NEUTRON SOURCE

The expected peak and average neutron flux values for the reference (1 MW) SNS target system are shown in Table 2 for moderators that are coupled, and both decoupled and poisoned. The SNS flux is about 6 times larger than that from (160 kW) ISIS and about 5 times smaller than that from the proposed (5 MW) European Spallation Source (ESS)[3]. In the present design the decoupling is accomplished by surrounding the moderator with 1 mm of cadmium. A 50-μm-thick gadolinium poison plate is placed in the center of the moderator parallel to the viewed moderator face. A comparison of the pulsed SNS neutron flux with the steady state values for HFIR and ILL is shown in Figure 4. During the early phase of the SNS neutron pulse, the generated flux is more than a factor of 10 brighter than that from reactors.

IV. VARIATION OF PULSE PARAMETERS WITH POISON PLATE LOCATION

The pulse width can be reduced by varying the location of the gadolinium poison plate. All results discussed above for a poisoned moderator have resulted from using a poison plate located in the center of the moderator (the plate is parallel to the viewed moderator face and equidistant between the viewed face and the face directly opposite). The effect that varying this location has on the neutron pulse from the moderator face is shown in Figure 5. To produce these results, we moved the plate from a location where the distance from the plate to the viewed moderator face was the total width divided by 8 (W/8 in the figure) to a location at the face opposite the viewed moderator face (W). This latter location is equivalent to having no poison since the effect of the poison is to reduce the moderator width as seen by low-energy (E_n<~0.3eV) neutrons. With no poison (W), the neutron intensity drops by less than two

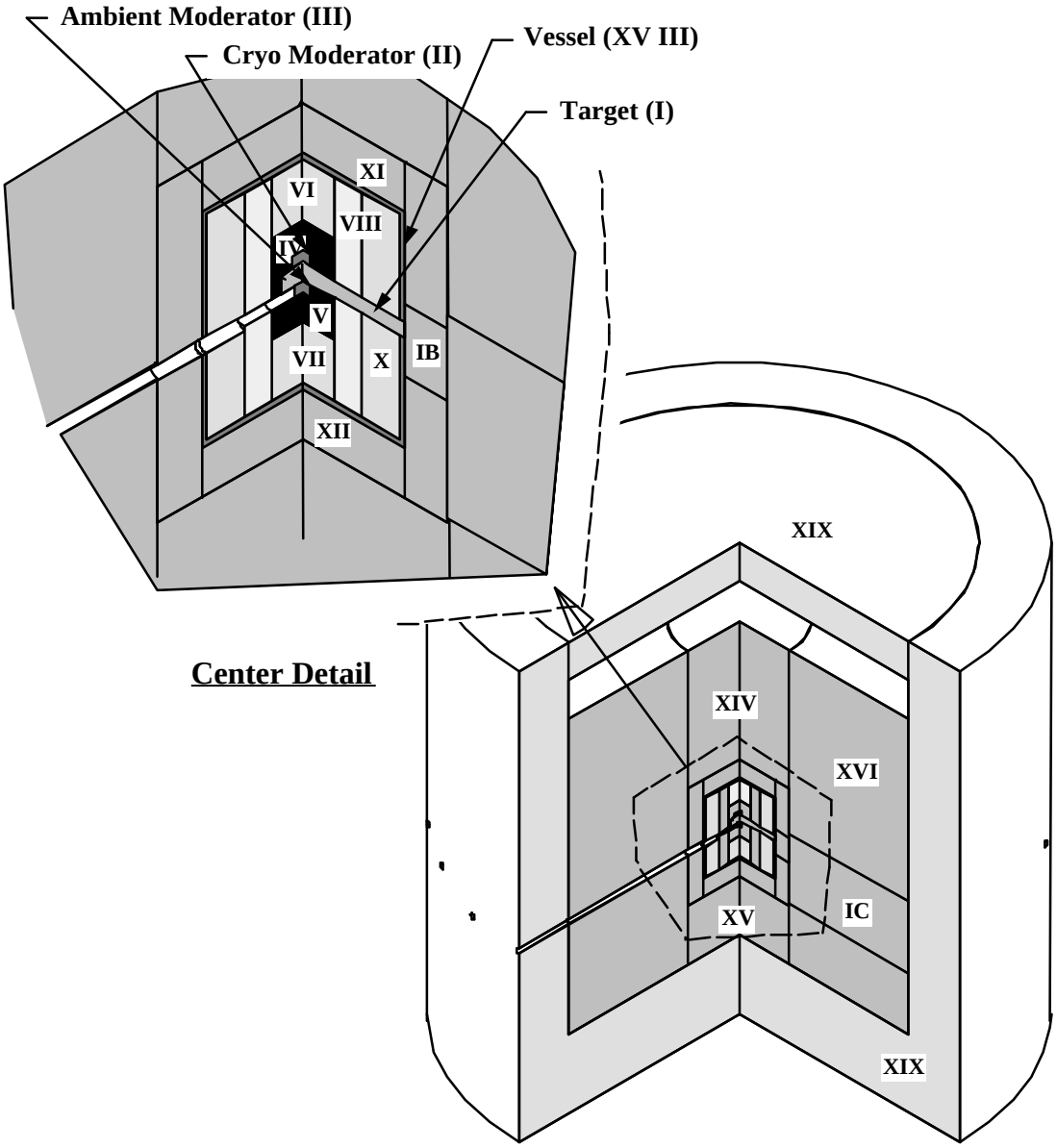

Figure 2. Schematic diagram of full target station model.

Table 1. Material Components for full target station model.

Sector		Description	Material
I		Target Assembly	
	A	Target	Mercury in water cooled shroud
	B	Intermediate Section	Mercury in Water Cooled Shield
	C	Outer Sector	Mercury in Water Cooled Shield
II		Cryogenic Moderator	Liquid Hydrogen in vacuum container
III		Ambient Moderator	Water filled SST box
IV		Upper, Inner Reflector	SST box with D2O Beryllium rods
V		Lower Inner Reflector	SST box with D2O Beryllium rods
VI		Upper, Outer Reflector Plug	SST box with D2O Nickel rods
VII		Lower Outer Reflector Plug	SST box with D2O Nickel rods
VIII		Upper Outer Reflector Ring	Cast Nickel Blocks with drilled cooling channels
IX		Lower Outer Reflector Ring	Cast Nickel Blocks with drilled cooling channels
X		Outer Reflector	Cast Nickel Blocks with drilled cooling channels
XI		Upper, Inner Shield Plug	Cast Iron Blocks with drilled cooling channels
XII		Lower, Inner Shield Plug	Cast Iron Blocks with drilled cooling channels
XIII		Inner Shield Ring	Cast Iron Blocks with drilled cooling channels
XIV		Upper, Outer Shield Plug	Cast Iron Blocks with drilled cooling channels
XV		Lower, Outer Shield Plug	Cast Iron Blocks with drilled cooling channels
XVI		Outer Shield Ring	Cast Iron Blocks with drilled cooling channels
XVII		Neutron Tube Plug	Sintered Tungsten Plug w/ cooling channels
XVIII		Vessel	Welded SST Vessel
	A		Cylinder
	B		Top
	C		Bottom
XIX		Concrete Shield	Conventional Poured Concrete
	A		Cylinder
	B		Top
	C		Bottom

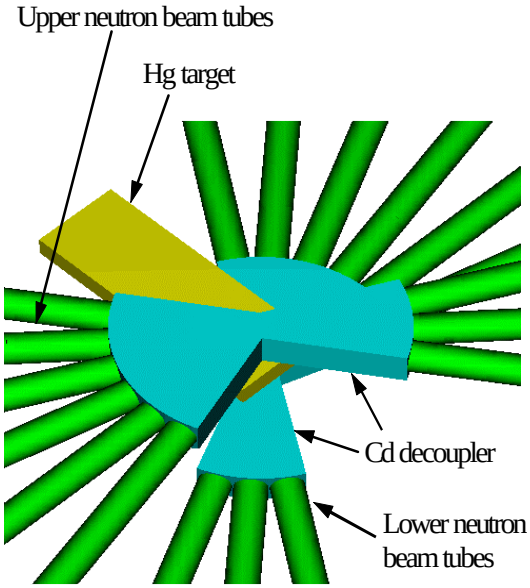

Figure 3. Full target station model with shielding and reflector assemblies removed.

Table 2. Peak and average neutron flux values for the viewed moderator faces (n/cm^2-s).

	H_2O Moderator		H_2 Moderator	
	coupled	decoupled/ poisoned	coupled	decoupled/ poisoned
Flux (peak) Flux (ave)	2.1×10^{16} 7.9×10^{13}	1.8×10^{16} 2.0×10^{13}	1.2×10^{16} 6.3×10^{13}	9.4×10^{15} 1.1×10^{13}

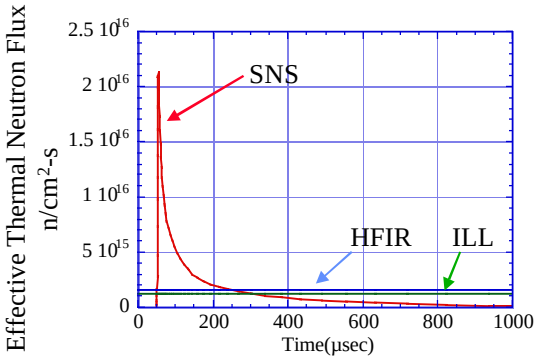

Figure 4. Expected performance of SNS compared to the HFIR and ILL reactors.

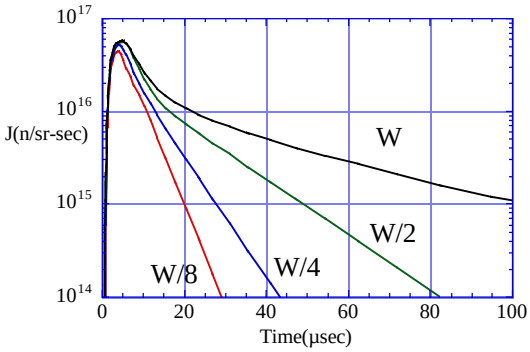

Figure 5. Neutron pulse (λ = 0.6 to 1.0 Å) for various locations of a gadolinium poison plate. The distance W is measured from the viewed moderator face (the width of the moderator is W).

orders of magnitude in 100 μs. With the poison at the other extreme (W/8), the neutron intensity drops by three orders of magnitude in 30 μs. Note that the peak neutron flux drops by only 20% from one extreme location of the plate to the other. Thus the poison plate location offers effective control over the pulse width with little change in the peak neutron intensity. The present recommended location for the poison plate is W/2, but further optimization will use the behavior shown in Figure 5 to better fit the moderator neutron output to the instrument needs.

V. TARGET MATERIAL TRADE STUDIES

Neutronic comparisons were made between tungsten, tantalum, and mercury target materials. The spectra of neutrons coming from the face of a H_2O moderator is shown in Figure 6 for each of these materials assuming 35% (by volume) cooling fraction of D_2O. The cooling is necessary for the two solid targets but is added in the case of mercury only for comparison. The neutron spectra for a mercury target with no assumed cooling fraction is also shown. The three materials are (within statistical uncertainties) equivalent when cooling is assumed. However when the unnecessary cooling is removed from the mercury target, mercury is clearly superior. Although not shown, the three materials are also equivalent when no cooling is assumed. Since the three materials are equivalent with the same cooling, and since the addition of cooling degrades the performance of all three materials it is clear that cooling requirements make mercury neutronically superior. The superiority of mercury increases with increases in power since progressively more cooling is required as the power is increased.

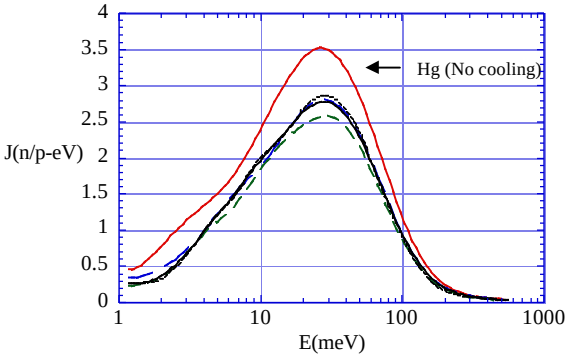

Figure 6. Neutron current from a H_2O moderator for various target materials: Mercury with no cooling (solid), Mercury with D_2O (long dashed), Tantalum with D_2O (short dashed), and Tungsten with D_2O (dotted).

VI. REFLECTOR MATERIAL TRADE STUDIES

Three different materials were considered for use as a neutron reflector. Nickel was easily excluded due to the greatly reduced neutron current through the moderator face compared to the other two. Lead (Pb) and beryllium (Be) remained candidates. The neutron pulse from a H_2 moderator when a Pb reflector is used and when a Be reflector is used is shown in Fig. 7. Results are shown in Fig. 8 for a H_2O moderator.

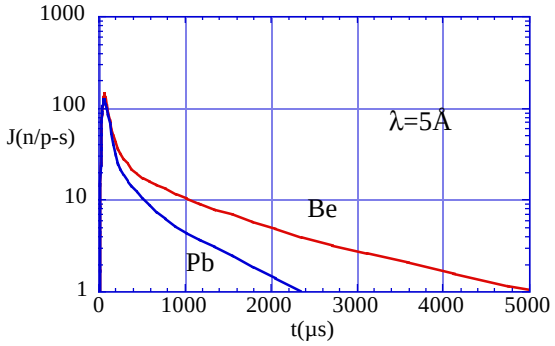

Fig. 7. Comparison:pulse from a H_2 moderator when a Be reflector is used and when a Pb reflector is used.

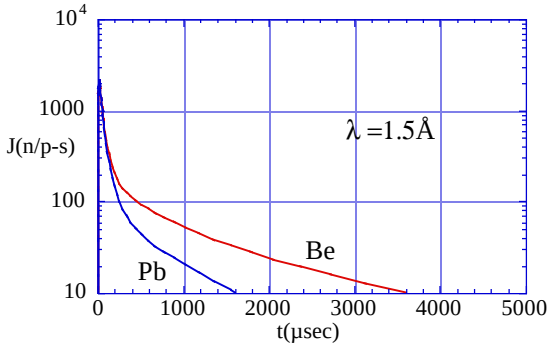

Fig. 8. Comparison:pulse from a H_2O moderator when a Be reflector is used and when a Pb reflector is used.

The pulse at a wavelength corresponding to the peak in the spectrum is shown in each case. The peak in the neutron output with time is about the same for the two materials. The time pulse width is narrower for the Pb reflector than for the Be reflector as is true for all wavelengths. This implies that there is a greater total neutron current in the case of Be. Thus, if total current is desired Be is the better material but if a narrow pulse is desired Pb is preferable. The trade-off between total current and the pulse width is, of course, something that should be determined on the basis of instrument requirements. However, a detailed study of the instrument requirements would be beyond the scope of the design study at this point. There exist several simple figures of merit (fom) that have been found to be useful [4,5,6,7] for quantitatively balancing the conflicting demands of maximizing the neutron current and minimizing the pulse width. The fom's used here have the form of neutron current divided by a time measure squared. Several time measures were used including the time full width at half maximum and the time width at 1/100 of maximum. The later is approximately the smallest neutron flux that would concern an experimentalist. A measure that puts in information about the full pulse is from Ref. 7 where the standard deviation of the pulse from its averaged value(Φ) was used as the time measure and was generally more highly weighted in our studies. The comparison between the fom's when a Pb and a Be reflector are used is shown in Table 3.

H2 Moderator(λ =5Å)

Refl. Mat.	$J/\Delta t_{1/2}^2$	$J/\Delta t_{1/100}^2$	J/σ^2
Be	2.8×10^{-3}	8.7×10^{-7}	8.7×10^{-5}
Pb	8.8×10^{-4}	2.5×10^{-6}	2.1×10^{-4}

H2O Moderator(λ =1.5Å)

Refl. Mat.	$J/\Delta t_{1/2}^2$	$J/\Delta t_{1/100}^2$	J/σ^2
Be	3.3×10^{-3}	1.2×10^{-6}	9.6×10^{-5}
Pb	2.1×10^{-3}	3.4×10^{-6}	3.2×10^{-4}

$\sigma^2 = \langle t^2 \rangle - \langle t \rangle^2$

Table 3.-Figure of Merit Comparison-Be vs. Pb Reflectors.

The comparison is again made at a wavelength corresponding to the peak in the spectrum from each moderator. Be was found to be better if the FWHM was used as the time measure but Pb was better if the width at 1/100 maximum was used or if Φ was used. Since a higher weight was place on Φ, Pb was judged to be neutronically better. Since other factors (such as reflector cost) also favored Pb it is the present choice for the SNS reflector. The design is being developed in such a way that if future considerations (such as detailed instrument studies) strongly suggest Be is better, the target station design could be changed without severe modifications.

VII. MODERATOR POSITION

In order to study the optimum moderator position and size we used a simple model (see Fig. 1). The simple model contained a mercury target with a rectangular cross section but with dimensions approximating those of the initial target model. Four moderators were used. In accordance with the present requests of the instrument designers, both H_2O moderators and the upstream H_2 moderator were decoupled and poisoned. The downstream H_2 moderator was coupled and unpoisoned. A Be reflector of equivalent size to the initial target model was used. It was found that the pulse width was roughly independent of the moderator location and thus only the neutron current needed to be considered when optimizing the neutron output. In Figs. 9 and 10 the neutron current is shown as a function of the distance (L) of the center of the moderators from the front of the Hg target. The

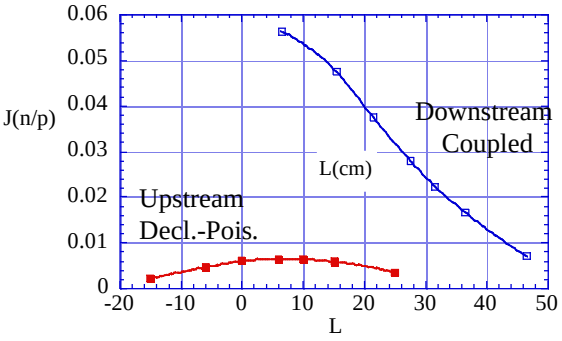

Fig. 9. Thermal neutron current from H_2 moderators.

Fig. 10. Thermal neutron current from H_2O moderators.

separation was maintained at 21.5 cm. For the H_2 moderators (Fig. 9), the upstream current peaked when the front of the moderator was at the front of the Hg target (L=6 cm). The current in the downstream moderator increased monotonically as the moderator moved upstream. The much smaller upstream current is due to the decoupling and poisoning which not only decreases the pulse width but also decreases the current. The current in the upstream moderator also peaks for the upstream H_2O moderators (Fig. 10) when the upstream edge of the moderator is at the upstream edge of the Hg, and the current in the downstream moderator also increases monotonically as the moderator moves toward the upstream edge of the Hg. Since both H_2O

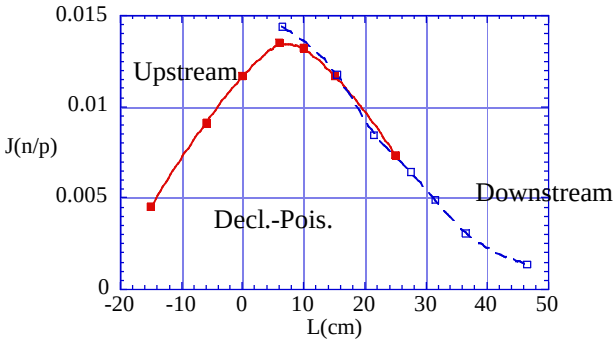

moderators are decoupled and poisoned the current is equal when they are at the same position.

Since there are 12 neutron beam tubes coming from the front moderators and only 6 from the back it was desirable to maximize the current in the front moderators independent of the back. This is accomplished by placing them with their upstream edges at the upstream edge of the Hg. After the optimization of the upstream moderators, the current from the downstream moderators are optimized by placing the moderators as close to the front as possible. This procedure could fail, however, if the location of one of the moderators has a large effect on the other. This question is addressed in Fig. 11 where the variation in the current in the downstream moderator is plotted as a function of L both when the front moderator is present (i.e., with moderator interaction) and when it isn't (i.e., with no moderator interaction).

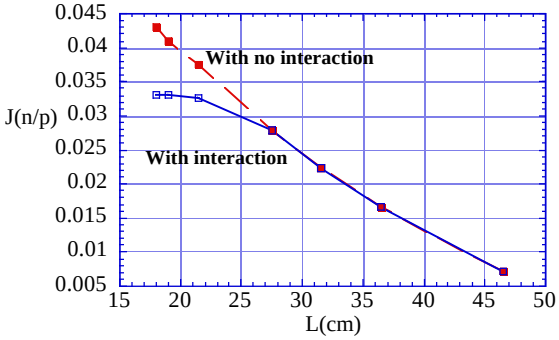

Fig. 11. Effect of moderator interaction on downstream coupled H_2 moderator output. Upstream moderator is a decoupled poisoned H_2O moderator located at L=6cm.

As may be seen, the presence of the front moderator reduces the current in the back moderator when they are close together (due to a decrease in the nearby reflector volume) but it doesn't cause a decrease in the current as the back moderator is moved forward. It is still desirable to have the back moderator as close to the front as possible. Thus the above optimization procedure is still valid.

VIII. PREMODERATOR STUDY

A premoderator used together with a cryogenic moderator can be very useful in reducing the heat deposited in the moderator material. This reduces demands on the cryogenic system and allows it to be made more simply and smaller. This reduction, in turn, can allow the active moderator material to be placed closer to the source and thus give a larger useful neutron flux.

The model geometry shown in Fig. 12 was used for the premoderator study reported here.

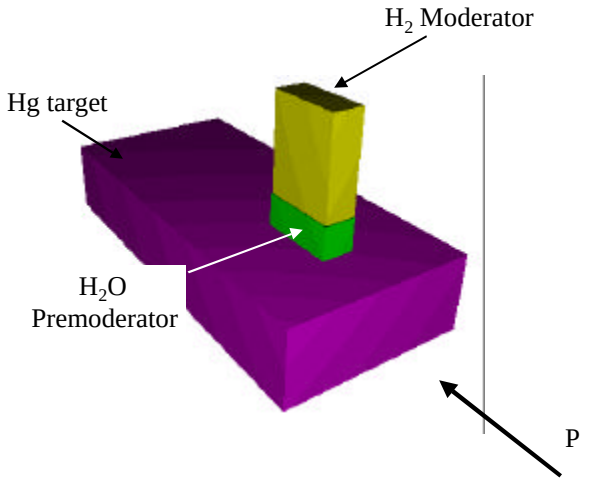

Fig. 12. Model geometry used for the premoderator study.

A H_2O premoderator was placed between the target and the cryogenic H_2 moderator. The size of the premoderator in the plane parallel to the target surface was the same as that of the moderator. The thickness (distance from the side of the premoderator next to the surface of the target to the side of the premoderator next to the moderator itself) was varied to assess the premoderator performance. With zero premoderator thickness the model geometry was identical to that used for the moderator position study discussed earlier.

Both the thermal neutron current and the energy deposition in the moderator are shown vs. premoderator thickness in Fig. 13. As the thickness is increased, there is first an increase in the current and then a decrease along with a continuous decrease in the energy deposition. Both are normalized to unity when no premoderator is present. The decrease in the current (expressed as a fraction of the the zero thickness current) is a good deal less than the decrease in the energy deposition (also expressed as a fraction of the zero thickness energy deposition). The energy deposition

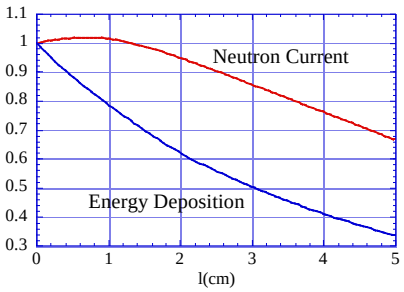

Fig. 13. Thermal neutron current and energy deposition vs the premoderator thickness(l).

(and thus the cost of the cryogenic system) can be decreased by a large amount with a much smaller decrease in the neutron current. A 3 cm premoderator can reduce the energy deposition by 50% with only a 15% loss of neutron current. A 3 cm premoderator is being incorporated into the SNS cryogenic H_2 moderator design.

In Fig. 14 the neutron spectra with no premoderator is shown along with the ratio of the current when a 5 cm premoderator is used to that when no premoderator is

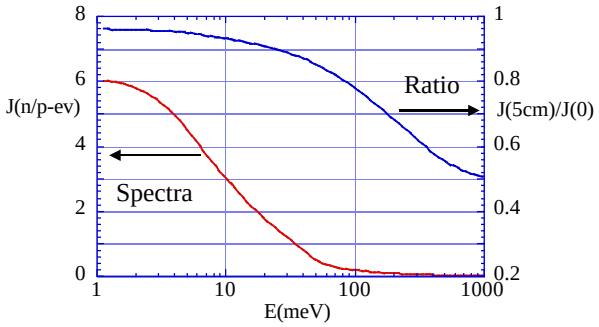

used.

Fig. 14.- Spectra with no premoderator and the ratio of the spectra with no premoderator and a 5 cm premoderator.

The current loss at an energy corresponding to the peak in the spectra is very small (5%) even with the large premoderator. The thermal current loss shown in the previous figure comes mainly from higher energy neutron loss. As the energy is increased, the current loss

reaches 10% at ~30 meV which is the approximate energy at the peak in the spectra from a H_2O moderator. Thus appreciable loss occurs only for neutrons which would be better obtained from a H_2O moderator. The penalty, in terms of current loss, is very small for neutrons in the energy range that would normally be obtained from a cryogenic H_2 moderator.

IX. SUMMARY AND CONCLUSIONS

The neutronics design and optimization analyses are now in progress to support initial selection of target system design features, materials, geometry, and component sizes for the proposed SNS. Initial optimization studies involving moderator poison plate location, target material performance, reflector performance, moderator position and moderator performance with the use of a premoderator for the target system have been performed. Preliminary results indicate first that a mercury target is neutronically better than tungsten or tantalum, especially at the higher (>1 MW) power levels where the solid targets need significant cooling water. Second, as measured by a simple figure of merit, Pb makes a better reflector than Be or Ni. Third, if it is desired that the upstream moderator be optimized independently of the downstream then the upstream edge of the upstream moderator should be at the upstream edge of the Hg. The downstream moderator is then optimized by placing it as close to the upstream as possible. Fourth, moving the poison plate has a strong effect (~ factors of 2 to 3) on the neutron pulse width and only a modest effect (~20%) on the neutron pulse intensity. Fifth, the use of a premoderator allows the energy deposition in a cryogenic H_2 moderator to be greatly decreased with little penalty in neutron current loss at energies where a H_2 moderator would normally be used. Finally, the targets used in this study were an "initial try" in a design study for SNS and do not represent a final configuration. It is anticipated that the results found, however, will have a very general applicability to the final design, and the "lessons" learned will apply in finding the best target configuration.

REFERENCES

1. T. A. Gabriel et. al., "CALOR87: HETC87, MICAP, EGS4, and SPECT, A Code System for Analyzing Detectors for Use in High Energy Physics Experiments," Proceedings of the Workshop on Detector Simulation for the SSC, ANL, Aug. 24-28, 1987.

2. J. F. Briesmeister, Ed., "MCNP-A General Purpose Monte Carlo Code for Neutron and Photon Transport," LASL Report LA-7396-M, Rev. 2, Sept. 1986.

3. "The European Spallation Source Study," Final Report 22, ESS-96-53-M, Jan. 1997.

4. C. G. Windsor, "Pulsed Neutron Scattering," Halsted Press, 1981.

5. D. H. Day and R. N. Sinclair, Nucl. Inst. Meth. Vol. 72, p. 237, 1969.

6. A. Michaudon, Reactor Science and Technology Vol. 17, p. 165, 1963

7. G. J. Russell, P. A. Seeger and R. G. Fluharty, "Parametric Studies of Target/Moderator Configurations for the Weapons Neutron Research (WNR) Facility," Los Alamos Report LA-6020, 1977.